Design of bandwidth enhanced and multiband MIMO antennas using characteristic modes

Miers, Zachary; Li, Hui; Lau, Buon Kiong

Published in:
IEEE Antennas and Wireless Propagation Letters

DOI:
10.1109/LAWP.2013.2292562

2013

Document Version:
Peer reviewed version (aka post-print)

Design of Bandwidth Enhanced and Multiband MIMO Antennas Using Characteristic Modes

Zachary Miers, *Student Member, IEEE*, Hui Li, *Member, IEEE*, and Buon Kiong Lau, *Senior Member, IEEE*

***Abstract*—Recent work has shown that, with the help of the Theory of Characteristic Modes (TCM), minor modifications of the terminal chassis can facilitate the design of orthogonal MIMO antennas with viable bandwidth at frequencies below 1 GHz. Herein, a new framework is proposed to further exploit TCM to enhance the performance of the orthogonal MIMO antennas. By correlating the characteristic currents and near fields of modes with high modal significance in a given frequency band, a single feed may be designed to excite multiple modes, leading to enlarged bandwidth. Similarly, the correlation of characteristic currents and near fields across different bands provides candidate modes that can be excited for multiband operation using a single feed. Moreover, the impedance matching of these modes can be improved by additional structural manipulation. As proof of concept, a dual-band (818-896MHz, 1841-2067MHz), dual-antenna prototype was designed on a 130 mm × 66 mm chassis for LTE operation. Full-wave simulation results were experimentally verified with a fabricated prototype.**

***Index Terms*—Antenna array, antenna design, MIMO systems, mutual coupling, mobile antenna.**

I. Introduction

The deployment of multiple-input multiple-output (MIMO) technology in Long Term Evolution (LTE) has greatly increased the complexity of antenna design in compact terminal devices, due to the requirement of implementing multi-antennas for a given frequency band within a limited space allocation [1]. In particular, the design challenge is severe at cellular bands below 1 GHz (e.g., 700 MHz LTE bands). At these frequencies, the antenna elements are electrically small and invariably rely on the terminal chassis to radiate efficiently. The sharing of the chassis as a radiator by multi-antennas results in strong mutual coupling, which commonly leads to reduced total efficiency and high correlation, and hence poor MIMO performance.

Recent studies have shown that chassis induced coupling can be mitigated by using the Theory of Characteristic Modes (TCM) [2] to select the location and/or radiation properties of the antenna elements on the chassis [3]-[5]. However, the underlying principle of these strategies is to only allow one antenna to exploit the chassis as a radiator, which limits the radiation properties of other antenna(s) in terms of bandwidth.

Manuscript received October 15, 2013. This work was supported in part by VINNOVA under grant no. 2009-04047, and in part by Vetenskapsrådet under grants no. 2010-468 and 2012-4859.

Z. Miers, H. Li, and B. K. Lau are with the Department of Electrical and Information Technology, Lund University, 221 00 Lund, Sweden (e-mail: {Zachary.Miers, Hui.Li, Buon_Kiong.Lau}@eit.lth.se).

One approach to achieve low coupling as well as reasonable bandwidth is to exploit multiple characteristic modes of the chassis for radiation. However, this concept was only proven at frequencies above 1 GHz [6], since only one characteristic mode is resonant for typical chassis sizes, e.g. 120 mm × 60 mm [7]. Moreover, the excitation of each mode in [6] requires multiple feed elements and a sophisticated matching network.

More recently, it was found that intentional but minor modification of the chassis (e.g., adding bezel ring or metal strips along the sides [7], [8]) can create additional resonant modes at frequencies below 1 GHz. These modes were then fed separately to realize orthogonal MIMO antennas [8], [9]. However, the initial work does not consider important aspects such as bandwidth enhancement and multiband operation, which are crucial for modern terminal application.

In this letter, we propose a new design framework to achieve wider bandwidth and multiband resonance for the MIMO antenna concept in [7]-[9]. The framework is based on the correlation of characteristic currents and near fields (of the electric and magnetic fields), which has been used to track a given characteristic mode across frequencies (see e.g., [10]). However, instead of tracking a given mode, we use the idea to identify other modes that have similar current characteristics in the vicinity of two or more feed locations determined using TCM [9]. The aim is make opportunistic use of existing feeds to excite additional mode(s) at a different frequency. Once the candidate modes are selected, appropriate chassis modification can be used to improve the impedance matching of these modes. For bandwidth enhancement, the chosen frequency for correlation should be close to the original frequency for multimode resonance, whereas the frequency spacing is larger for obtaining multiband resonances. To demonstrate these concepts, a dual-band, dual-antenna prototype was designed on a 130 mm × 66 mm chassis for LTE operation, and simulation results agree well with measured results.

II. Characteristic Mode Modification Below 1 GHz

To illustrate the design framework, a mobile phone chassis with dimensions 130 mm × 66 mm (typical for smartphones) was analyzed using TCM [2]. The first five characteristic modes are tracked by correlating the characteristic currents of each individual mode over frequency [10], producing the curves in Fig. 1. The structure supports only one resonant mode below 1 GHz, which we will refer to as the fundamental chassis mode. This mode has the same current distribution as that of a dipole along the length of the chassis [3].

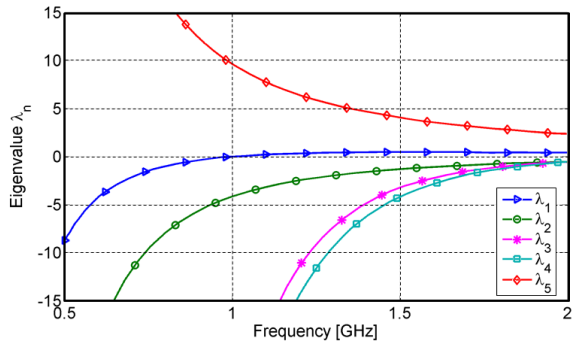

Fig. 1. Characteristic eigenvalues for a 130 mm × 66 mm chassis.

The basic planar structure supports two eigenmodes with values between ±5 at 900 MHz; λ_1 is the fundamental mode supporting a dipole current distribution along the length of the chassis, λ_2 supports a current distribution matching that of a dipole along the width of the chassis. To reduce resonant frequency of λ_2, the structure can be capacitively loaded along the sides of the chassis. An example realization of capacitive loading with metal strips is depicted in Fig. 2(a) [8]. This chassis modification lowers the resonant frequency of λ_2 as well as creates new modes that were not originally supported in the planar structure. Figure 3 shows that this simple modification allows the structure to support three resonant modes below 1 GHz. The mode λ_2 is now denoted as λ_1, whereas the fundamental chassis mode is now λ_3, numbered by the order of zero-crossing.

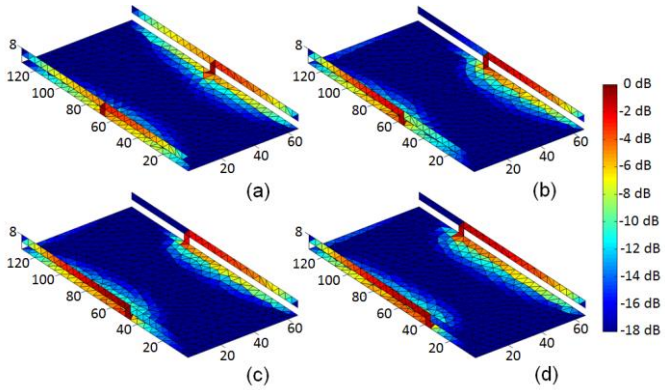

Fig. 2. Normalized current distribution of λ_1 on a 130 mm × 66 mm chassis with the addition of an 8 mm high capacitive loading structure with shorting pins (a) centered along the length of the structure, (b) at 10 mm rotationally symmetric offset, (c) at 20 mm rotationally symmetric offset, (d) at 30 mm rotationally symmetric offset.

The characteristics of a fat dipole allow for the capacitance to be varied by offsetting the placement of the shorting pins while maintaining the short dipole's characteristic currents. Using TCM, it is observed that mode λ_1 can be tuned in the same way. This modification allows the resonance of λ_1 to be tuned from 950 to 650 MHz when the shorting pins are moved from the center of the structure (Fig. 2(a)) to a 30 mm rotationally symmetric offset (Fig. 2(d)).

The feed for λ_1 can be placed at a high current location, which is the shorting pin for all cases in Fig. 2. Through removing one of the two shorting pins and placing a feed port at this location, the modal characteristics of the structure will remain unchanged. On the other hand, λ_3 can be excited by an electric antenna positioned at one short edge [3]. An electric antenna is one that predominantly radiates electric field in the near field region [4].

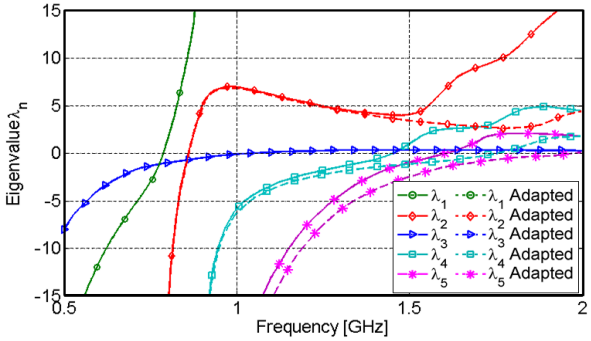

Fig. 3. The first five eigenvalues of the modified chassis with shorting pins at 22 mm rotationally symmetric offset. Adapted modes were formed through shortening the shorter ends of the capacitive strips by 10 mm.

III. Multimode Bandwidth Enhancement

Though λ_1 can be tuned over a wide frequency range, it only supports a limited bandwidth, as can be expected from its abrupt zero crossing in Fig. 3. Using an L matching network and feeding only λ_1 without changing the structure, a limited bandwidth of around 6% can be realized. To enhance the bandwidth for cellular band coverage, the characteristics of λ_2 (of Fig. 3) were analyzed. The currents, near fields, and patterns show λ_2 supports a mode of operation resembling that of an open-ended slot antenna with its resonant frequency dependent on the length of the slot. This mode was found to be tunable independently of the location of the shorting pin and therefore does not adversely affect the tuning characteristics of λ_1. As the length of the capacitive loading strip is shortened, the resonant frequencies of both λ_1 and λ_2 are increased, with the resonant frequency of λ_2 increasing at a much higher rate than that of λ_1. This allows the resonant frequencies of λ_1 and λ_2 to be tuned separately.

The feeding of two separate modes in an effort to increase bandwidth is not always realizable as the ideal feeding types, locations, and impedances may greatly vary from one another. To understand the benefits and drawbacks of purposefully exciting two separate modes with a single feed to increase bandwidth, the characteristic currents and near fields of the two modes were correlated with each other. In these two modes, the currents and near fields are significantly decorrelated across the entirety of the chassis. However, the areas around the capacitive strips are significantly more correlated. Each mode jointly supports a strong characteristic current at the shorting pins, with significantly high correlation in the magnitude of the electric fields in the vicinity of the capacitive strip. These similarities allow the structure to support simultaneous excitation of both λ_1 and λ_2 through a single feed located at one of the two shorting pins, which extends the structure's bandwidth potential. The tunability of the two modes is accomplished through the use of the shorting pin location and length of the longer arm of the capacitive strip. Using these modifications, it is possible to tune the resonance from 650 MHz to beyond 1 GHz, while maintaining simultaneous excitation of both modes, as shown in Fig. 4.

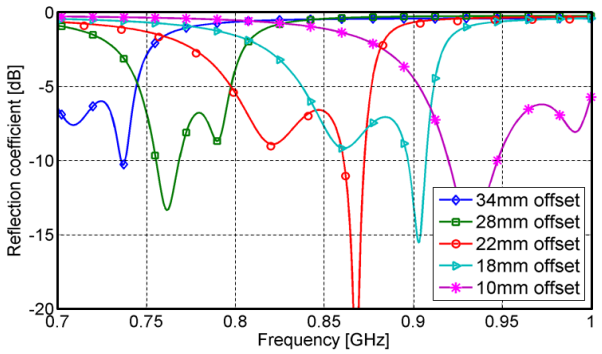

Fig. 4. Tunability of the enhanced bandwidth structure through excitation of two modes by changing the rotationally symmetric offset (in mm) of the two shorting pins from the center position. The capacitive strip remains a constant length of 130 mm without any additional tuning of the longer arm.

For practicality, this antenna was tuned to cover LTE bands 5, 6, and 19 as these are widely used LTE bands below 1 GHz. This is achieved by applying a 22 mm rotationally symmetric offset to the shorting pins and reducing the longer arm of the capacitive strip by 5 mm. The tuned structure supports a total bandwidth from 820-900 MHz, covering all three LTE bands.

IV. Multi-Band Resonance

By correlating the characteristic currents of a given band with those of other frequencies around the original feeding locations, it is possible to further manipulate the chassis to achieve multi-band performance using the same feeds. To illustrate this concept, we designed a dual-band version of the tuned structure in Section III, so as to cover LTE bands 5, 6, and 19 as well as LTE band 2 (1850-1990 MHz), as the latter is one of the more widely used LTE bands above 1 GHz.

The first five characteristic modes of the tuned structure in Section III were shown earlier in Fig. 3. For any current mode, it is possible to cross correlate specific locations of a structure between modes at different frequencies. Using these correlations, higher frequency modes that can potentially be excited using the existing feeding structures can be found. Following this procedure, the currents around the shorting pins and capacitive loading strips at the resonances of λ_1 and λ_2 were cross-correlated with characteristic currents of modes ($\lambda \epsilon \pm 30$) that form between 1.3-2.0 GHz. Two modes within 1.3-2.0 GHz (i.e., λ_2 and λ_4) showed significantly high correlation between the feed locations in the low band and those at higher frequencies. Neither of the two modes is resonant near 1.8 GHz (see Fig. 3). However, due to their modal currents and low eigenvalues, these two modes can potentially be fed using the existing feeding structure.

Once these two modes were selected for further evaluation, the entire structure was evaluated for correlation between the low frequency currents in λ_1 and λ_2 and the higher frequency λ_2 and λ_4 currents. The currents were found to be significantly decorrelated from one another along the length of the capacitive strips. The decorrelation is due to the structure exhibiting high modal current densities along the shorter ends of the strips in the high frequency modes, and low current densities in these same locations in the low frequency modes. It is possible to modify the structure without any significant impact to the modes at locations where the current density is near zero. In contrast, small structural modifications in areas of large current density will have a significant impact on these modes of operation. Due to the largely decorrelated current densities along the capacitive strips, both strips were shortened along their shorter ends. As the strips were shortened, the eigenvalues λ_2 and λ_4 decrease substantially (i.e., become more resonant) around 1800 MHz, as seen in the "adapted modes" in Fig. 3. In contrast, the lower frequency modes where not significantly impacted by the shortened strips.

Accordingly, by adjusting the length of the shorter ends of the strips, it is possible to adjust the resonance of λ_4 from 1.4 GHz to beyond 3 GHz. However, due to the L matching network used to match the low band, the correct impedance match must be adapted for use in the higher band. The L network used in the bands below 1 GHz utilized a parallel inductor and series capacitor; this type of tuning indicates that the system will be best matched to the structural impedance if the impedance is inductive. Fortunately, both modes were inductively mismatched (positive eigenvalues) above 1.75 GHz. However, if a capacitive structural impedance was required, additional structural modifications could be utilized to force this structural impedance at the required location.

V. Full-Wave Simulation Verification

The proposed antenna system was implemented into a full wave model and simulated using the frequency domain finite element method (FEM) solver of CST Microwave Studio. The fundamental chassis mode (λ_3) was excited using the coupling element proposed in [1], which was added to the structure from Section IV. In an effort to use industry-acceptable materials in a cost-effective manner, the antenna was adapted for fabrication on a polycarbonate carrier. The polycarbonate material (ε_r=2.27 tan δ=0.012) loads both the fundamental mode and the orthogonal mode, such that minor re-tuning of the structure was needed. Specifically, the capacitance at the ends of the capacitive loading plates was reduced by tapering the strip width, whereas the fundamental mode was re-tuned by increasing the separation distance between the coupling elements and the chassis. The final design is shown in Fig. 5.

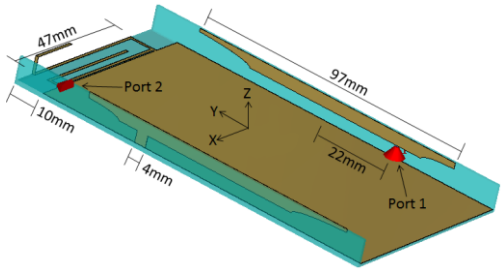

Fig. 5. Final simulated prototype with the total dimensions 130 mm × 66 mm × 8 mm chassis and a 20 mm rotationally symmetric capacitive loading offset.

Both the fundamental mode port (port 1) and the orthogonal mode port (port 2) were matched using the BetaMatch software [12]. To match the high band of the port 1, a single 1.0pF Marata capacitor was used. To match port 2, a two-element L matching network consisting of a 4.3nH parallel inductor and a 5.0pF series capacitor was used. The final

design produced 6 dB impedance bandwidths of 818-896 MHz and 1841-2067 MHz in the low and high bands, respectively. The average far-field envelope correlation coefficient (ECC) for both bands as calculated from the antenna patterns (assuming uniform 3D angular power spectrum) was below 0.05. An average total efficiency of -1.2 dB was achieved in port 1 and -1.6 dB in port 2 within the low band. The average total efficiency of the high band was -1.2 dB in port 1 and -0.9 dB in port 2. The simulated S parameters are shown in Fig. 6.

VI. Prototype Verification

The proposed antenna system was fabricated and is shown in Fig. 7. The corresponding S parameters are given in Fig. 6. The far-field patterns and total efficiencies of the antennas were measured in a SATIMO Stargate system (see Fig. 8). These patterns correspond well with the simulated patterns. The measured patterns show that a high level of orthogonality is achieved between the two ports in both the low and high bands. The ECC calculated from the measured patterns (assuming uniform 3D angular power spectrum) were below 0.1 across both bands, which is slightly higher than the simulated values. The discrepancy can be attributed to cabling, fabrication tolerance, and practical difficulties in measuring low correlation. The average measured efficiency of both antennas was -1.5dB from 820-900MHz. In the high band, the measured efficiencies were -1.5dB and -0.9dB for ports 1 and 2, respectively.

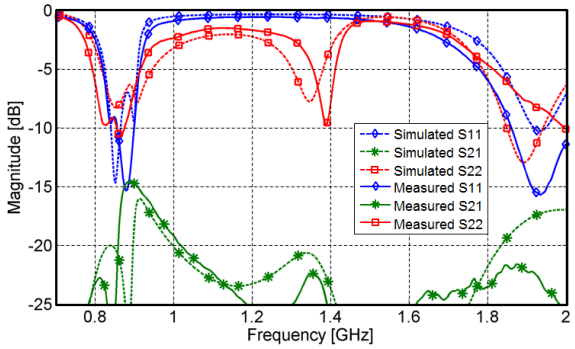

Fig. 6. S parameters of the CST simulated and measured prototype of the dual band orthogonal antennas designed using the TCM .

Fig. 7. 130mm x 66mm x 8mm fabricated polycarbonate chassis with 20mm rotationally symmetric capacitive loading offset.

VII. Conclusion

In this work, a new and practical framework to design multiband MIMO terminal antennas with viable bandwidth was presented. By correlating characteristic currents of a given structure across different frequencies, orthogonal modes of similar current distributions can be identified and excited at a different frequency with existing feeds. Using this method, both bandwidth enhancement and multiband resonances can be achieved. An illustrative design example was presented and the simulation results were verified in measurements.

Acknowledgment

The authors would like to thank Lite-On Mobile AB for their help in measuring the prototype's antenna patterns.

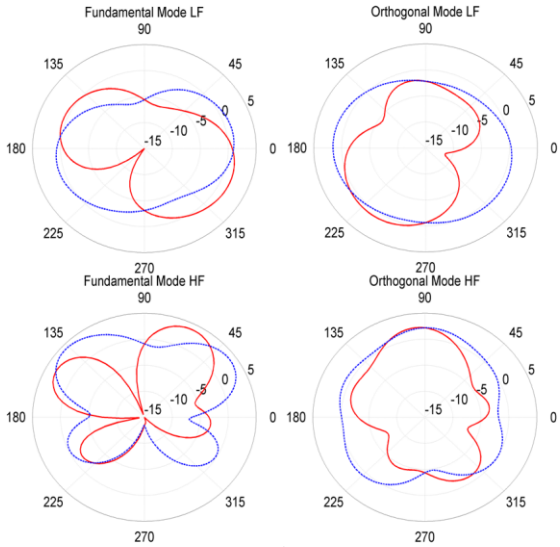

Fig. 8. Measured radiation patterns of the dual-band dual-antenna prototype in both low frequency (LF) and high frequency (HF) bands. Solid red lines are the X-Y principal plane while dashed blue lines are the Y-Z principal plane.

References

[1] B. K. Lau, "Multiple antenna terminals," in *MIMO: From Theory to Implementation*, C. Oestges, A. Sibille, and A. Zanella, Eds. San Diego: Academic Press, 2011, pp. 267-298.

[2] R. F. Harrington and J. R. Mautz, "Computation of characteristic modes for conducting bodies," *IEEE Trans. Antennas Propag.*, vol. AP19, pp. 629-639, Sep. 1971.

[3] H. Li et al., "Characteristic mode based tradeoff analysis of antenna-chassis interactions for multiple antenna terminals," *IEEE Trans. Antennas Propag.*, vol. 60, pp. 490-502, Feb. 2012.

[4] H. Li, B. K. Lau, Z. Ying, and S. He, "Decoupling of multiple antennas in terminals with chassis excitation using polarization diversity, angle diversity and current control," *IEEE Trans. Antennas Propag.*, vol. 60, pp. 5947-5957, Dec 2012.

[5] H. Li et al., "Impact of current localization on the performance of compact MIMO antennas," in *Proc. 5th Europ. Conf. Antennas Propag. (EuCAP'2011)*, Rome, Italy, Apr. 11-15, 2011, pp. 2423-2426.

[6] D. Manteuffel and R. Martens, "Multiple antenna integration in small terminals," in *Proc. Int. Symp. Antennas Propag. (ISAP'2012)*, Nagoya, Japan, Oct.29-Nov.2, 2012, pp. 211-214.

[7] H. Li, Z. Miers, and B. K. Lau, "Generating multiple characteristic modes below 1GHz in small terminals for MIMO antenna design," in *Proc. IEEE Int. Symp. Antenna Propag. (APSURSI'2013)*, Orlando, FL, USA, Jul. 7-13, 2013.

[8] H. Li, Z. Miers, and B. K. Lau, "Design of orthogonal MIMO handset antennas based on characteristic mode manipulation at frequency bands below 1 GHz," *IEEE Trans. Antennas Propag.*, in revision.

[9] Z. Miers, H. Li, and B. K. Lau, "Design of multi-antenna feeding for MIMO terminals based on characteristic modes," in *Proc. IEEE Int. Symp. Antennas Propag. (APSURSI'2013)*, Orlando, FL, Jul. 7-13, 2013.

[10] M. Capek, P. Hazdra, P. Hamouz, and J. Eichler, "A method for tracking characteristic numbers and vectors," *Progress In Electromagnetics Research B*, vol. 33, 115-134, 2011

[11] K.-J. Kim et al., "Small antenna with a coupling feed and parasitic elements for multiband mobile applications," *IEEE Antennas Wireless Propag. Lett.*, vol. 10, pp. 290–293, 2011

[12] MNW Scan Pte Ltd, BetaMatch. [Online]. Available: http://http://www.mnw-scan.com